

Published in final edited form as:

Hepatology. 2011 January ; 53(1): 106–115. doi:10.1002/hep.23998.

Osteopontin is Induced by Hedgehog Pathway Activation and Promotes Fibrosis Progression in Nonalcoholic Steatohepatitis

Wing-Kin Syn^{1,2}, Steve S Choi^{1,3}, Evaggelia Liaskou², Gamze F Karaca¹, Kolade M Agboola¹, Ye Htun Oo², Zhiyong Mi⁴, Thiago A Pereira^{1,5}, Marzena Zdanowicz¹, Padmini Malladi⁶, Yuping Chen¹, Cynthia Moylan^{1,3}, Youngmi Jung^{1,7}, Syamal D. Bhattacharya⁴, Vanessa Teaberry¹, A Omenetti¹, Manal F. Abdelmalek¹, Cynthia D Guy⁸, David H Adams², Paul C Kuo⁴, Gregory A Michelotti¹, Peter F Whittington⁶, and Anna Mae Diehl¹

¹Division of Gastroenterology, Department of Medicine, Duke University Medical Center, Durham, NC, USA

²Centre for Liver Research and NIHR Biomedical Research Unit, University of Birmingham, Edgbaston, Birmingham, UK

³Section of Gastroenterology, Department of Medicine, Durham Veteran Affairs Medical Center, Durham, NC, USA

⁴Department of Surgery, Duke University Medical Center, Durham, NC, USA

⁵Nucleo de Doencas Infecciosas, Centro de Ciencias da Saude, Universidade Federal do Espirito Santo, Espirito Santo, Brazil

⁶Department of Pediatrics, The Feinberg School of Medicine, Northwestern University, Children's Memorial Institute for Education and Research, Chicago, Illinois, USA

⁷Department of Biological Sciences, Pusan National University, Pusan, Korea

⁸Department of Pathology, Duke University Medical Center, Durham, NC, USA

Abstract

Background—Nonalcoholic steatohepatitis (NASH) is a leading cause of cirrhosis. Recently, we showed that NASH-related cirrhosis is associated with Hedgehog (Hh) pathway activation. The gene encoding Osteopontin (OPN), a pro-fibrogenic extracellular matrix protein and cytokine, is a direct transcriptional target of the Hh pathway. Thus, we hypothesized that Hh signaling induces OPN to promote liver fibrosis in NASH.

Methods—Hepatic OPN expression and liver fibrosis were analyzed in wild-type (WT) mice, Patched-deficient (Ptc^{+/-}) (overly-active Hh signaling) mice, and OPN-deficient mice before and after feeding methionine-choline deficient (MCD) diets to induce NASH-related fibrosis. Hepatic OPN was also quantified in human NASH and non-diseased livers. Hh signaling was manipulated in cultured liver cells to assess direct effects on OPN expression, and hepatic stellate cells (HSC) were cultured in medium with different OPN activities to determine effects on HSC phenotype.

Results—When fed MCD diets, Ptc^{+/-} mice expressed more OPN and developed worse liver fibrosis (p<0.05) than WT mice, while OPN-deficient mice exhibited reduced fibrosis (p<0.05). In NASH patients, OPN was significantly up-regulated and correlated with Hh pathway activity and

Corresponding Author: Anna Mae Diehl, MD Florence McAlister Professor & Chief Division of Gastroenterology Duke University Snyderman Bldg., Suite 1073 595 LaSalle Street Durham, NC 27710 Tel: 919-684-4173 or 919-684-2616 Fax: 919-684-4183 diehl004@mc.duke.edu.

Conflict of Interest:

Authors declare no conflict of interest

fibrosis stage. During NASH, ductular cells strongly expressed OPN. In cultured HSC, SAG (a Hh agonist) upregulated, while Cyclopamine (a Hh-antagonist) repressed, OPN expression ($p < 0.005$). Cholangiocyte-derived OPN and recombinant OPN promoted fibrogenic responses in HSC ($p < 0.05$); neutralizing OPN with RNA-aptamers attenuated this ($p < 0.05$).

Conclusions—OPN is Hh-regulated and directly promotes pro-fibrogenic responses. OPN induction correlates with Hh pathway activity and fibrosis-stage. Therefore, OPN inhibition may be beneficial in NASH.

Keywords

hedgehog; non-alcoholic fatty liver disease; osteopontin

Introduction

NASH is a potentially serious form of chronic liver injury because it increases the risk of developing cirrhosis and primary liver cancer. The mechanisms that lead to these outcomes have not been fully elucidated, but appear to involve responses that are triggered by hepatocyte apoptosis (1,2) and myofibroblast accumulation (3). Certain apoptotic stimuli were recently reported to induce hepatocyte production of Hedgehog (Hh ligands) (4). Hh ligands, in turn, elicit a number of fibrogenic actions by engaging their receptors on Hh-responsive liver cells, such as ductular type cells, hepatic stellate cells (HSC) and natural killer T (NKT) cells. In HSC, for example, Hh pathway activation functions in a cell-autonomous fashion to promote transition of quiescent (Q)-HSC to myofibroblastic (MF)-HSC, enhance MF-HSC proliferation, and inhibit MF-HSC apoptosis (5). Activating Hh signaling in other types of liver cells (e.g., ductular cells and NKT cells) also causes these cells to generate factors that promote MF-HSC accumulation by paracrine mechanisms (6,7).

Osteopontin (OPN), a pro-inflammatory cytokine and integrin-binding ligand (8-10), is highly expressed in many inflamed tissues and plays a critical role in wound healing (11-13). Recently, Glioblastoma (Gli) binding sites were demonstrated in the OPN promoter, prompting speculation that Hh signaling might regulate OPN transcription (14). This concept is potentially relevant to NASH-related liver fibrosis because Hh pathway activity increases in parallel with fibrosis stage in NASH. Moreover, in other tissues, OPN is secreted by the types of cells (e.g., NKT cells and fibroblasts) that mediate fibrogenic repair in NASH (15,16). Evidence that OPN mRNAs increase during culture-related activation of Q-HSC to MF-HSC (16) and correlate with fibrosis severity in biliary atresia (17) further support a potential role for OPN in cirrhosis pathogenesis. Therefore, we manipulated Hh pathway activity in mice and cultured cells to determine effects on OPN production, and examined whether or not reducing OPN impacted Hh signaling or fibrogenesis. The results support and advance the concept that OPN is a Hh-target gene and reveal a previously-unsuspected role for OPN as a proximal mediator of Hedgehog's fibrogenic actions in NASH.

Materials and Methods

Animals

C57BL/6 Patched-deficient ($Ptc^{+/-}$) mice were obtained from Dr. R.J. Wechsler-Reya (Duke University, NC), and wild-type mice (WT) were obtained from Jackson Laboratories (Bar Harbor, ME). $Ptc^{+/-}$ mice have only 1 copy of patched, a Hh-pathway repressor. Therefore, these mice are unable to silence Hh signaling and exhibit excessive Hh-pathway activity. WT and $Ptc^{+/-}$ mice were fed the methionine-choline- deficient (MCD) diet to

induce nonalcoholic steatohepatitis (NASH) and liver fibrosis or control chow (n= 8/group) for 8 weeks. 129 Sv/J Black-Swiss OPN-deficient (OPN^{-/-}) mice or littermate controls were also fed the MCD or control chow (n = 6 / group) Because the 129 Sv/J strain was reported to be more sensitive to MCD treatment than the C57Bl/6 strain (18), OPN^{-/-} mice and littermate controls were fed the diets for 4, rather than 8, weeks.

Animal care and procedures were approved by the Duke University and Northwestern University Institutional Animal Care and Use Committees as set forth in the “Guide for the Care and Use of Laboratory Animals” published by the National Institutes of Health.

Histopathologic Analysis

Serial sections were stained with H&E. NAFLD severity was assessed using criteria described by Brunt et al (19) (Supplementary Materials/Methods). To quantify liver fibrosis, five micron sections were stained with picosirus red (Sigma, St. Louis, MO) and counterstained with fast green (Sigma, St. Louis, MO). Collagen stained with Sirius Red was quantitated in the sections that were randomly chosen (under 20X magnification, 10 fields each from sample), as described (20).

Immunohistochemistry

To localize and characterize cells that produce and/or respond to Hh ligands and OPN, formalin-fixed, paraffin-embedded (FFPE) livers were prepared for immunohistochemistry as described (6,7). Protocols and antibodies used are listed in Supplementary Materials/Methods and Supplementary Table 1.

Molecular Techniques

Real-time reverse-transcription polymerase chain reaction (RT-PCR) and Western immunoblot were performed using established protocols (7); details are in Supplementary Materials/Methods and Supplementary Table 2.

Isolation and culture of primary rodent stellate cells

Hepatic stellate cells (HSC) were isolated from normal Sprague-Dawley rats as previously described (21) (Supplemental Materials/Methods). A similar isolation/culture protocol was used for studies involving mouse primary HSC (6). Day 4 HSC were used in all experiments.

Human HSCs

The human HSC line, LX-2, was cultured in serum-supplemented DMEM. Primary human HSC were isolated as previously described (21).

Studies of Hh and OPN in cultured HSC

To evaluate the effects of Hedgehog-signaling on HSC, day 4 HSC cultures were grown for an additional 24 h in medium containing either exogenous Hedgehog agonist (SAG) at a concentration of 0.3uM, 5uM cyclopamine (Toronto Research Chemicals Inc., Toronto, Canada), an inhibitor of Hh-signaling, or 5uM tomatidine (Calbiochem, San Diego, CA), a catalytically inactive analog of cyclopamine (5,21) (tomatidine serves as a control for cyclopamine).

In separate experiments, recombinant OPN (rOPN) or vehicle was added to cultures to assess their effects on HSC activation. 100ng/ml dose was used in this study because it stimulated greatest effects in vitro (22). The effects of inactivating OPN was subsequently assessed by treating HSC with human OPN RNA aptamer OPN-R3 or its biologically-

inactive mutant, OPN-R3-2 (both synthesized by Dharmacon, Lafayette, CO) (23). Aptamers (100 nmol/l) were added to medium for 48 hours prior to harvest. This concentration of OPN aptamer has been shown to inhibit adhesion, migration and invasion in the MDA-MB-231 breast cancer cell line (which highly expresses OPN and is a standard tool for evaluating OPN actions) (23).

All cell experiments were performed at least in duplicate. Total RNA and protein were harvested before and at the end of the treatments, and analyzed by QRT-PCR and immunoblotting, respectively.

Effect of cholangiocyte-conditioned media on primary HSC activation

The immortalized, but non-transformed, murine immature cholangiocyte cell line, 603B was maintained in 6-well, cell-culture plates (Costar 3516, Corning Incorporated) in standard culture media as previously described (24,25). At 90% confluence, cholangiocyte-conditioned media were harvested and added to primary HSC cultures together with OPN-targeted RNA aptamers or null-aptamers; HSC were harvested 2 days later and mRNA expression was analyzed by QRT-PCR. Experiments were performed in duplicate wells and repeated twice.

Human liver studies

FFPE liver sections from de-identified controls and subjects with biopsy-proven NASH, and explanted liver tissues from individuals undergoing liver transplantation for NASH or ASH-cirrhosis (n=6/group) from the Liver and Hepatobiliary Unit, Birmingham, UK and Department of Pathology at Duke University were used. Normal tissues were obtained from non-diseased livers removed during resection for colorectal hepatic metastases or from split-liver grafts.

Freshly explanted autoimmune hepatitis, primary sclerosing cholangitis, and primary biliary cirrhosis-cirrhotic liver tissues were also snap-frozen and used for total liver RNA analyses.

All studies using material from Duke University Hospital were conducted in accordance with NIH and Institutional guidelines for human subject research. Studies of samples acquired from the Hepatobiliary Unit in Birmingham were done in accordance with local ethical approval 04/Q2708/41 and REC 2003/242 from the South-Birmingham Research Ethics Committee, UK (Supplemental Materials/Methods and Supplemental Table 1).

Statistical Analysis

The results are expressed as mean \pm SEM. Statistical significance was determined using Student's t test. Significance was accepted at the 5% level, *P < 0.05.

Results

Up-regulation of Osteopontin (OPN) parallels Hh pathway activation during methionine-choline deficient (MCD) diet-induced Nonalcoholic Steatohepatitis (NASH)

WT mice (n=8/group) develop hepatic necro-inflammation, accumulate markers of myofibroblastic (MF)-HSC, and exhibit liver fibrosis after 8 weeks of MCD diet. Ptc^{+/-} mice (with haplo-insufficiency of Ptc, a factor that constrains Hh signaling) exhibit worse liver fibrosis than WT mice after MCD diet exposure (Fig 1A, Suppl Fig 1A-D) (6,7). This suggests that Hh pathway activation promotes fibrosis progression in this model of NASH, but the exact mechanisms involved need to be determined.

Hh pathway activation results in nuclear accumulation of Gli proteins (downstream targets of Hh signaling) (26), and Gli proteins may regulate transcription of OPN, a potential pro-fibrogenic factor (27-29). Therefore, we compared OPN expression in WT mice that were fed either control or MCD diets for 8 weeks. In WT mice, MCD diets caused a significant induction of OPN mRNA (>10-fold) and protein (about 2-fold) expression (Fig 1B-C, Suppl Fig 1E). *Ptc*^{+/-} mice exhibited even greater up-regulation of OPN expression when fed MCD diets (Fig 1B-C, Suppl Fig 2A-B). The latter finding supports the concept that Hh signaling increases OPN expression.

In both strains, the OPN-immunoreactive cells were mostly ductular in appearance (Fig 1D). Double immunostaining for Gli2 and OPN in liver samples from NASH patients demonstrated that Gli2-(+) ductular cells that co-expressed OPN localized within fibrous septae (Fig 1E).

MCD diet-fed OPN-deficient mice developed less fibrosis

To evaluate whether or not OPN directly contributed to the fibrogenic response evoked by MCD diets, and gain further insight into the relationship between OPN and the Hh pathway, *OPN*^{-/-} mice (n=12) and littermates (n=12) were fed MCD or control diets for 4 weeks. OPN deficiency had no obvious effect on expression of the Hh-target gene, *Gli2*, because both *OPN*^{-/-} and littermates showed similar induction of *Gli2* mRNA (data not shown) and protein (Fig 2A) after 4 weeks of MCD diet. Despite apparent similarities in Hh pathway activity, however, the fibrogenic responses of *OPN*^{-/-} mice were markedly attenuated when compared to that of their littermate controls. After MCD diet feeding, for example, *OPN*^{-/-} mice accumulated 50% fewer α SMA⁺ cells (Fig 2B) and significantly fewer Sirius red stained fibrils (Fig 2C) than comparably-treated littermates. These results are consistent with an earlier report of reduced collagen gene expression in *OPN*^{-/-} mice (18), and suggest that the Hh pathway mediates its fibrogenic effects, at least in part, by inducing expression of OPN.

Paracrine/Autocrine OPN stimulates HSC expression of fibrogenic phenotype

Hh-responsive bile ductular cells are major sources of OPN (Fig 1E). Therefore, we treated primary cultures of rodent HSC with conditioned medium from monocultures of a cholangiocyte cell line, and assessed effects on HSC gene expression. To determine if HSC responses were mediated by OPN, studies were repeated using cholangiocyte-conditioned medium plus OPN-targeted aptamers. Cholangiocyte-conditioned media augmented HSC expression of α -sma (Fig 3A) and collagen (Fig 3B); RNA-aptamer treatment repressed α -sma induction by 50% and returned collagen expression to basal values, proving that paracrine signaling involving OPN promoted fibrogenic gene expression in HSC. In separate studies, other primary HSC cultures were treated with recombinant OPN (rOPN, 100ng/ml) or vehicle for 24 hours, and RNA was analyzed by QRT-PCR (Fig 3C-D). rOPN also augmented expression of α sma (Fig 3C), and collagen Ia1 expression (Fig 3D). These findings support the concept that exogenous OPN can function as a paracrine factor to promote fibrogenic gene expression in HSC.

Because another group has reported that MF-HSC themselves also express OPN (16), we next investigated changes in endogenous OPN gene expression during “spontaneous” culture-related activation of Q-HSC to MF-HSC. We confirmed that HSC expression of OPN mRNA and protein increased significantly as Q-HSC transitioned to become MF-HSC (Fig 4A, Suppl Fig 3A). Addition of OPN aptamers to day 4 cultures significantly repressed α -sma and collagen gene expression, providing novel evidence that HSC-derived OPN may help to maintain the myofibroblastic phenotype of cultured HSC. As HSC become MF, they repress expression of the Hh inhibitor, *Hhip*, induce expression of Hh ligands, and up-

regulate various MF genes, while down-regulating markers of quiescence (5). To clarify the relationship between Hh pathway activation and OPN expression, day 4 culture-activated MF-HSC were treated with cyclopamine to selectively inhibit Hh signaling. Cultures were harvested 24 h later, RNA was isolated, gene expression was assessed by QRT-PCR, and results were compared to parallel cultures that had been treated with tomatidine, an inactive cyclopamine analog. Inhibiting Hh signaling with cyclopamine attenuated induction of OPN gene expression (Fig 4B, Suppl Fig 4B). Conversely, addition of the Hh agonist, SAG, augmented OPN gene expression significantly (Fig 4C). Thus, endogenous OPN gene expression in MF-HSC is regulated, at least in part, by the Hh pathway.

To determine the relative importance of OPN as a down-stream target of the Hh pathway in HSC, day 4 primary MF-HSC from *Ptc*^{+/-} mice were incubated with OPN-aptamers for 48 hours. At baseline, HSC from *Ptc*^{+/-} mice expressed 3-fold more *gli2* mRNA than WT HSC, confirming that *Ptc*-deficiency enhances Hh signaling (Fig 5A). Consistent with *in vivo* findings (Fig 1), *Ptc*^{+/-} HSC also expressed more OPN mRNA than WT HSC (Fig 5B). Neutralizing OPN significantly reduced collagen and α -sma mRNA levels in the *Ptc*-deficient HSC (Fig 5C-D), but had little effect on *gli2* mRNA expression (Fig 5E). These findings suggest that the Hh pathway mediates induction of certain fibrogenic genes indirectly, via up-regulation of the Hh-responsive gene OPN.

Evidence of OPN over-expression in humans with progressive NAFLD

Because the mouse model of MCD diet-induced NASH differs in several regards from human NASH (30), it was important to determine if OPN over-expression occurred in patients with NAFLD. Coded liver sections from 11 patients with well-characterized NAFL (*n* = 3), NASH (*n* = 3), and NASH-related cirrhosis (*n*=5) were stained to demonstrate OPN, and then analyzed by computer-assisted morphometry. Expression of OPN was lowest in patients with NAFL and highest in patients with NASH-cirrhosis (Fig 6A-B). To further validate the association between NAFLD-fibrosis stage and OPN expression, total liver RNA was isolated from a separate cohort of 36 individuals with early (Fibrosis stage F0-1) or advanced (F3-4) NASH-fibrosis (*n*=18/group) and analyzed by QRT-PCR. In livers with advanced -fibrosis OPN gene expression was double that of livers with early fibrosis (Fig 6C). Additional analysis was conducted using RNA and protein harvested from explanted livers with NASH-cirrhosis and residual tissue from non-diseased donor livers (*n*=6 per disease). Livers with NASH-cirrhosis contained over 10x more OPN protein (Fig 6D, Suppl Fig 4) and 5x more OPN mRNA compared with non-diseased controls (Fig 7A). Interestingly, OPN was also significantly increased in livers from individuals with ALD-cirrhosis (Fig 7A, B, Suppl Fig 4), primary biliary cirrhosis (PBC) (Fig 7A, C), autoimmune hepatitis (AIH), and primary sclerosing cholangitis (PSC) (Fig 7A), suggesting that OPN induction is a conserved response to chronic liver injury.

Discussion

Cirrhosis rarely occurs unless NAFL progresses to NASH, a condition that is characterized by inflammation and hepatocyte death (31). However, only a minority of individuals with NASH actually develop cirrhosis. Fibrosis stage in NASH has been shown to correlate with the level of hepatic apoptotic activity (1,32). Index liver biopsies of NASH patients who eventually become cirrhotic also harbor more myofibroblasts (MF) than those who do not (3). These observations link hepatocyte apoptosis with MF accumulation and fibrosis progression in NASH.

There is further evidence that phagocytosis of apoptotic debris stimulates HSC to become MF (33). Recently, we identified a potentially related mechanism by which hepatocyte apoptosis promotes MF accumulation and liver fibrosis by demonstrating that dying

hepatocytes produce Hh ligands (4). Biologically active Hh ligands are detected in apoptotic fragments released by ligand-producing cells (34). Hh ligands, in turn, engage various types of Hh-responsive cells, including HSC, ductular-type cells, and NKT cells, to trigger fibrogenic responses (7,35,36). Consistent with these findings, we observed that Hh activity correlated with MF accumulation and fibrosis stage in NAFLD patients and rodent models of NAFLD, and suggested that inter-individual differences in Hh signaling influenced intensity of fibrogenic responses during NASH (7). The present studies provide further support for this concept because they identify OPN as a proximal effector of Hh-mediated fibrogenesis, and demonstrate that livers of OPN-deficient mice are significantly protected from NASH-related fibrosis.

A recent analysis of the OPN gene revealed binding sites for Gli transcription factors, suggesting that OPN transcription is likely to be regulated by Hh signaling (14). By demonstrating co-localization of Gli and OPN in liver cells, and proving that expression of OPN mRNA is increased by a Smoothed agonist, but decreased by a Smoothed antagonist, our results support and advance this concept. In addition, our data demonstrate that changes in OPN gene expression are paralleled by changes in OPN protein content and biological activity because OPN aptamers reverse the pro-fibrogenic actions of OPN. The latter studies also verify that OPN is a significant down-stream target of Hh signaling (rather than vice versa) because neutralizing OPN had no effect on cellular expression of the Hh-target gene, Gli2, but significantly diminished fibrogenic gene expression, even in Ptc-deficient cells with supra-normal Hh pathway activity. Coupled with the evidence that OPN $-/-$ mice are significantly protected from NASH-related fibrosis, the data explain why we noted that hepatic content of Gli2(+) cells and OPN (+) cells increased in parallel as liver fibrosis advanced in patients with NAFLD.

Although the present studies focused on the roles of OPN as a paracrine factor for cholangiocyte-stellate cell fibrogenic interactions, and an autocrine mediator of fibrogenic gene expression in MF-HSC, other cell types might also contribute to the fibrogenic actions of OPN in NASH. NKT cells are particularly noteworthy in this regard. These liver-enriched immune cells are capable of producing and responding to Hh ligands (35), and are also known to secrete OPN (15). To our knowledge, the possibility that Hh signaling might regulate OPN expression in NKT cells has not been evaluated. However, we previously demonstrated that Hh pathway activation enhances hepatic accumulation of NKT cells (6). We and others (6,37) also showed that hepatic NKT cell content is significantly increased in patients with NASH-related cirrhosis. Moreover, activated liver NKT cells generate soluble factors that evoke expression of fibrogenic genes in cultured HSC, and mice that are genetically deficient in NKT cells are relatively protected from NASH-related fibrosis (6), similar to OPN-deficient mice.

Therefore, OPN induction may represent a conserved pro-fibrogenic mechanism among several distinct types of Hh-responsive liver cells, including ductular cells, MF-HSC, and NKT cells. Such reasoning suggests that inter-individual differences in OPN production may contribute to differences in the outcomes of NASH. Indeed, OPN may also dictate the fibrogenic response in other chronic liver diseases, as it is significantly overexpressed in livers from cirrhotic ALD, AIH, PBC and PSC, and a recent study reported that plasma OPN levels correlate with hepatic inflammation and fibrosis in chronic hepatitis C (38). Although more work is needed to delineate the interactions between OPN and other putative pro-fibrogenic factors (39), this concept suggests that OPN levels may provide a useful biomarker for liver fibrosis in NASH, and that OPN-neutralization might be useful for preventing progressive hepatic fibrosis in NASH patients.

Supplementary Material

Refer to Web version on PubMed Central for supplementary material.

Acknowledgments

Authors would like to thank Dr R.J. Wechsler-Reya (Duke University Medical Center, NC) for providing the Patched-deficient (Ptc^{+/-}) mice, Dr. G. J. Gores (Mayo Clinic, Rochester, MN) and Yoshiyuki Ueno (Tohoku University, Sendai, Japan) for providing the murine immature ductular cell line (603B), Dr M Rojkind (George Washington University Washington, DC) for providing the rat hepatic stellate cell (HSC) line 8B, and Dr Scott L Friedman (Mount Sinai School of Medicine, NY) for providing the human HSC line, LX-2. We are grateful to Dr Mari Shinohara (Duke University Medical Center, NC) and Dr T Uede (Hokkaido University, Japan) for helpful discussions.

In addition, the authors thank Dr Jiawen Huang for his assistance with animal care and Mr. Carl Stone for administrative support.

Funding:

Majority of work was supported grants from the National Institute of Health, RO1 DK053792 and RO1 DK077794 to AMD, with contributions from the Medical Research Council, Wellcome Trust, EU and NIH 5R01AA14257-5 to DHA, and EASL Fellowship to WKS.

Abbreviations

α-sma	alpha-smooth muscle actin
FFPE	formalin-fixed paraffin embedded
Gli	glioblastoma
Hh	Hedgehog
HSC	hepatic stellate cell
NAFLD	nonalcoholic fatty liver disease
NASH	nonalcoholic steatohepatitis
MCD	methionine choline deficient
OPN	osteopontin
OPN	osteopontin
Ptc	patched
Shh	sonic hedgehog
WT	wild type

References

1. Feldstein AE, Canbay A, Angulo P, Tanai M, Burgart LJ, Lindor KD, Gores GJ. Hepatocyte apoptosis and fas expression are prominent features of human nonalcoholic steatohepatitis. *Gastroenterology*. 2003; 125:437–443. [PubMed: 12891546]
2. Wieckowska A, Zein NN, Yerian LM, Lopez AR, McCullough AJ, Feldstein AE. In vivo assessment of liver cell apoptosis as a novel biomarker of disease severity in nonalcoholic fatty liver disease. *Hepatology*. 2006; 44:27–33. [PubMed: 16799979]
3. Feldstein AE, Papouchado BG, Angulo P, Sanderson S, Adams L, Gores GJ. Hepatic stellate cells and fibrosis progression in patients with nonalcoholic fatty liver disease. *Clin Gastroenterol Hepatol*. 2005; 3:384–389. [PubMed: 15822044]

4. Jung Y, Witek RP, Syn WK, Choi SS, Omenetti A, Premont R, Guy CD, et al. Signals from dying hepatocytes trigger growth of liver progenitors. *Gut*. 59:655–665. [PubMed: 20427400]
5. Choi SS, Omenetti A, Witek RP, Moylan CA, Syn WK, Jung Y, Yang L, et al. Hedgehog pathway activation and epithelial-to-mesenchymal transitions during myofibroblastic transformation of rat hepatic cells in culture and cirrhosis. *Am J Physiol Gastrointest Liver Physiol*. 2009; 297:G1093–1106. [PubMed: 19815628]
6. Syn WK, Oo YH, Pereira TA, Karaca GF, Jung Y, Omenetti A, Witek RP, et al. Accumulation of natural killer T cells in progressive nonalcoholic fatty liver disease. *Hepatology*. 51:1998–2007. [PubMed: 20512988]
7. Syn WK, Jung Y, Omenetti A, Abdelmalek M, Guy CD, Yang L, Wang J, et al. Hedgehog-mediated epithelial-to-mesenchymal transition and fibrogenic repair in nonalcoholic fatty liver disease. *Gastroenterology*. 2009; 137:1478–1488 e1478. [PubMed: 19577569]
8. Ashkar S, Weber GF, Panoutsakopoulou V, Sanchirico ME, Jansson M, Zawaideh S, Rittling SR, et al. Eta-1 (osteopontin): an early component of type-1 (cell-mediated) immunity. *Science*. 2000; 287:860–864. [PubMed: 10657301]
9. Chabas D, Baranzini SE, Mitchell D, Bernard CC, Rittling SR, Denhardt DT, Sobel RA, et al. The influence of the proinflammatory cytokine, osteopontin, on autoimmune demyelinating disease. *Science*. 2001; 294:1731–1735. [PubMed: 11721059]
10. Rangaswami H, Bulbule A, Kundu GC. Osteopontin: role in cell signaling and cancer progression. *Trends Cell Biol*. 2006; 16:79–87. [PubMed: 16406521]
11. Miyazaki K, Okada Y, Yamanaka O, Kitano A, Ikeda K, Kon S, Uede T, et al. Corneal wound healing in an osteopontin-deficient mouse. *Invest Ophthalmol Vis Sci*. 2008; 49:1367–1375. [PubMed: 18385052]
12. Fujita N, Fujita S, Okada Y, Fujita K, Kitano A, Yamanaka O, Miyamoto T, et al. Impaired angiogenic response in the corneas of mice lacking osteopontin. *Invest Ophthalmol Vis Sci*. 51:790–794. [PubMed: 19741245]
13. Lorena D, Darby IA, Gadeau AP, Leen LL, Rittling S, Porto LC, Rosenbaum J, et al. Osteopontin expression in normal and fibrotic liver. altered liver healing in osteopontin-deficient mice. *J Hepatol*. 2006; 44:383–390. [PubMed: 16221502]
14. Das S, Harris LG, Metge BJ, Liu S, Riker AI, Samant RS, Shevde LA. The hedgehog pathway transcription factor GLI1 promotes malignant behavior of cancer cells by up-regulating osteopontin. *J Biol Chem*. 2009; 284:22888–22897. [PubMed: 19556240]
15. Diao H, Kon S, Iwabuchi K, Kimura C, Morimoto J, Ito D, Segawa T, et al. Osteopontin as a mediator of NKT cell function in T cell-mediated liver diseases. *Immunity*. 2004; 21:539–550. [PubMed: 15485631]
16. Lee SH, Seo GS, Park YN, Yoo TM, Sohn DH. Effects and regulation of osteopontin in rat hepatic stellate cells. *Biochem Pharmacol*. 2004; 68:2367–2378. [PubMed: 15548383]
17. Whittington PF, Malladi P, Melin-Aldana H, Azzam R, Mack CL, Sahai A. Expression of osteopontin correlates with portal biliary proliferation and fibrosis in biliary atresia. *Pediatr Res*. 2005; 57:837–844. [PubMed: 15845635]
18. Sahai A, Malladi P, Melin-Aldana H, Green RM, Whittington PF. Upregulation of osteopontin expression is involved in the development of nonalcoholic steatohepatitis in a dietary murine model. *Am J Physiol Gastrointest Liver Physiol*. 2004; 287:G264–273. [PubMed: 15044174]
19. Brunt EM, Janney CG, Di Bisceglie AM, Neuschwander-Tetri BA, Bacon BR. Nonalcoholic steatohepatitis: a proposal for grading and staging the histological lesions. *Am J Gastroenterol*. 1999; 94:2467–2474. [PubMed: 10484010]
20. Yata Y, Gotwals P, Kotliansky V, Rockey DC. Dose-dependent inhibition of hepatic fibrosis in mice by a TGF-beta soluble receptor: implications for antifibrotic therapy. *Hepatology*. 2002; 35:1022–1030. [PubMed: 11981752]
21. Choi SS, Witek RP, Yang L, Omenetti A, Syn WK, Moylan CA, Jung Y, et al. Activation of Rac1 promotes hedgehog-mediated acquisition of the myofibroblastic phenotype in rat and human hepatic stellate cells. *Hepatology*. 52:278–290. [PubMed: 20578145]

22. Heilmann K, Hoffmann U, Witte E, Loddenkemper C, Sina C, Schreiber S, Hayford C, et al. Osteopontin as two-sided mediator of intestinal inflammation. *J Cell Mol Med.* 2009; 13:1162–1174. [PubMed: 18627421]
23. Mi Z, Guo H, Russell MB, Liu Y, Sullenger BA, Kuo PC. RNA aptamer blockade of osteopontin inhibits growth and metastasis of MDA-MB231 breast cancer cells. *Mol Ther.* 2009; 17:153–161. [PubMed: 18985031]
24. Yahagi K, Ishii M, Kobayashi K, Ueno Y, Mano Y, Niitsuma H, Igarashi T, et al. Primary culture of cholangiocytes from normal mouse liver. *In Vitro Cell Dev Biol Anim.* 1998; 34:512–514. [PubMed: 9719406]
25. Ishimura N, Bronk SF, Gores GJ. Inducible nitric oxide synthase up-regulates Notch-1 in mouse cholangiocytes: implications for carcinogenesis. *Gastroenterology.* 2005; 128:1354–1368. [PubMed: 15887117]
26. Omenetti A, Diehl AM. The adventures of sonic hedgehog in development and repair. II. Sonic hedgehog and liver development, inflammation, and cancer. *Am J Physiol Gastrointest Liver Physiol.* 2008; 294:G595–598. [PubMed: 18218671]
27. Mori R, Shaw TJ, Martin P. Molecular mechanisms linking wound inflammation and fibrosis: knockdown of osteopontin leads to rapid repair and reduced scarring. *J Exp Med.* 2008; 205:43–51. [PubMed: 18180311]
28. Morimoto J, Inobe M, Kimura C, Kon S, Diao H, Aoki M, Miyazaki T, et al. Osteopontin affects the persistence of beta-glucan-induced hepatic granuloma formation and tissue injury through two distinct mechanisms. *Int Immunol.* 2004; 16:477–488. [PubMed: 14978021]
29. Berman JS, Serlin D, Li X, Whitley G, Hayes J, Rishikof DC, Ricupero DA, et al. Altered bleomycin-induced lung fibrosis in osteopontin-deficient mice. *Am J Physiol Lung Cell Mol Physiol.* 2004; 286:L1311–1318. [PubMed: 14977630]
30. Larter CZ, Yeh MM. Animal models of NASH: getting both pathology and metabolic context right. *J Gastroenterol Hepatol.* 2008; 23:1635–1648. [PubMed: 18752564]
31. Syn WK, Teaberry V, Choi SS, Diehl AM. Similarities and differences in the pathogenesis of alcoholic and nonalcoholic steatohepatitis. *Semin Liver Dis.* 2009; 29:200–210. [PubMed: 19387919]
32. Canbay A, Higuchi H, Bronk SF, Taniai M, Sebo TJ, Gores GJ. Fas enhances fibrogenesis in the bile duct ligated mouse: a link between apoptosis and fibrosis. *Gastroenterology.* 2002; 123:1323–1330. [PubMed: 12360492]
33. Canbay A, Feldstein AE, Higuchi H, Werneburg N, Grambihler A, Bronk SF, Gores GJ. Kupffer cell engulfment of apoptotic bodies stimulates death ligand and cytokine expression. *Hepatology.* 2003; 38:1188–1198. [PubMed: 14578857]
34. Witek RP, Yang L, Liu R, Jung Y, Omenetti A, Syn WK, Choi SS, et al. Liver cell-derived microparticles activate hedgehog signaling and alter gene expression in hepatic endothelial cells. *Gastroenterology.* 2009; 136:320–330 e322. [PubMed: 19013163]
35. Syn WK, Witek RP, Curbishley SM, Jung Y, Choi SS, Enrich B, Omenetti A, et al. Role for hedgehog pathway in regulating growth and function of invariant NKT cells. *Eur J Immunol.* 2009; 39:1879–1892. [PubMed: 19544307]
36. Omenetti A, Porrello A, Jung Y, Yang L, Popov Y, Choi SS, Witek RP, et al. Hedgehog signaling regulates epithelial-mesenchymal transition during biliary fibrosis in rodents and humans. *J Clin Invest.* 2008; 118:3331–3342. [PubMed: 18802480]
37. Tajiri K, Shimizu Y, Tsuneyama K, Sugiyama T. Role of liver-infiltrating CD3+CD56+ natural killer T cells in the pathogenesis of nonalcoholic fatty liver disease. *Eur J Gastroenterol Hepatol.* 2009; 21:673–680. [PubMed: 19318971]
38. Huang W, Zhu G, Huang M, Lou G, Liu Y, Wang S. Plasma osteopontin concentration correlates with the severity of hepatic fibrosis and inflammation in HCV-infected subjects. *Clin Chim Acta.* 411:675–678. [PubMed: 20138033]
39. Fickert P, Thueringer A, Moustafa T, Silbert D, Gumhold J, Tsybrovskyy O, Lebofsky M, et al. The role of osteopontin and tumor necrosis factor alpha receptor-1 in xenobiotic-induced cholangitis and biliary fibrosis in mice. *Lab Invest.* 90:844–852. [PubMed: 20368698]

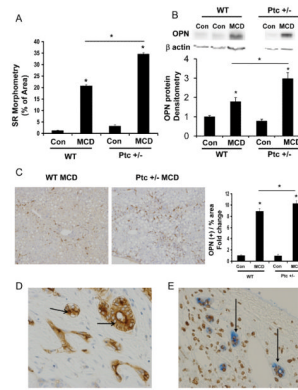


Figure 1. Osteopontin (OPN) expression parallels Hedgehog (Hh) pathway activation and fibrosis during diet-induced NASH

Wild-type and Ptc^{+/-} mice (with an overly active Hh pathway) were fed control chow (n=8/group) or MCD diet (n=8/group) for 8 weeks, and then sacrificed. (A) Sirius red quantification by morphometric analysis. Sections from 4 animals were used per group and 10 randomly selected, 200X fields chosen for analysis by the Metaview software. (B) Total hepatic OPN expression by Western blot and densitometry. (C) Representative OPN immunostaining after MCD treatment in WT and Ptc^{+/-} mice (final magnification 400X), and quantification by morphometry. Sections from 4 animals were used per group and 8 randomly selected, 200X fields chosen for analysis by the Metaview software. Results are expressed as fold change (% positive staining) relative to chow-fed control mice, and graphed as mean \pm SEM. *P<0.05 vs. control mice. (D) Representative OPN (+) biliary ductular cells in murine NASH-fibrosis (630X). (E) Representative OPN (blue) and Gli2 (brown) double-positive ductular cells in human NASH-cirrhosis (400X).

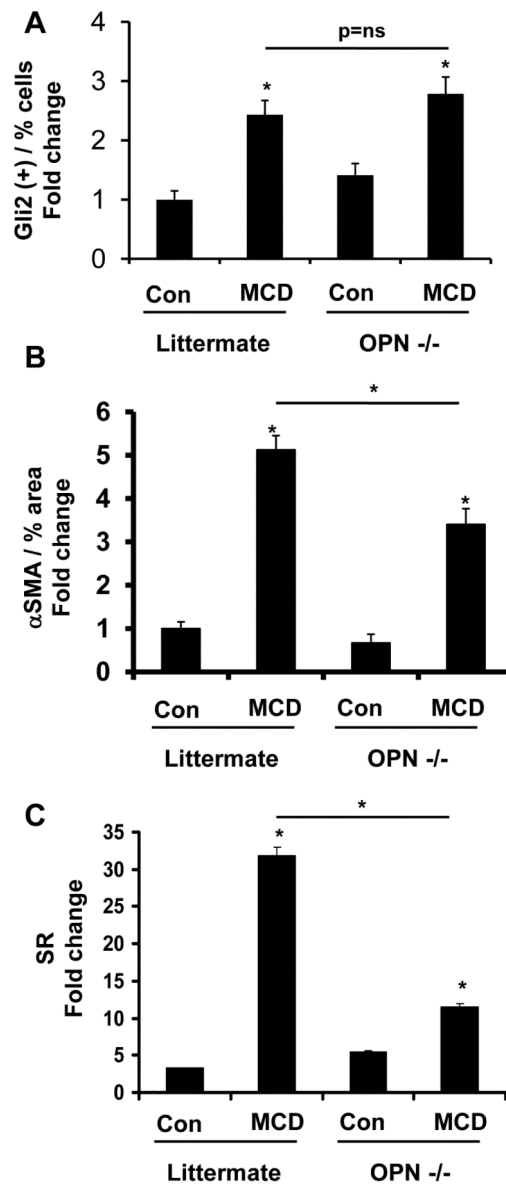


Figure 2. OPN-deficient mice develop less fibrosis after MCD diet treatment

129Sv/J OPN-deficient and littermates were fed MCD diet or control chow (n=6 mice/group/dietary treatment) for 4 weeks. At the end of treatment, mice were sacrificed. (A) Accumulation of Gli2 (+) cells in OPN^{-/-} and littermates. Sections from 6 animals were used, and 8 randomly selected, 400X field chosen for cell counting. (B) α SMA morphometry. Sections from 3 animals were used at each time point and 10 randomly selected, 400X fields chosen for analysis by the Metaview software. (C) Sirius red quantification by morphometric analysis. Sections from 6 animals were used and 10 randomly selected 400X field chosen for analysis. Results are expressed as fold change relative to chow-fed littermates and graphed as mean \pm SEM. *P<0.05 vs. littermate control.

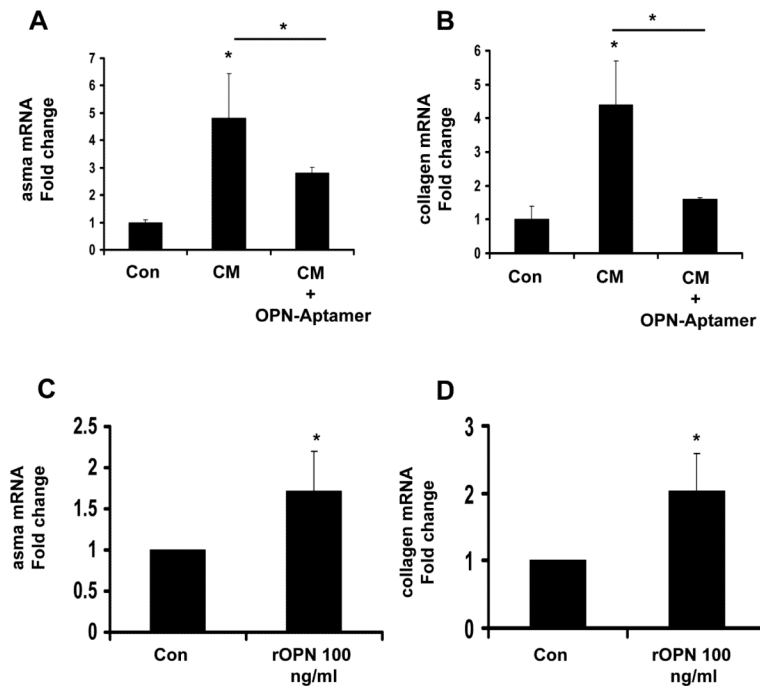


Figure 3. Paracrine OPN stimulates hepatic stellate cell (HSC) activation and collagen expression

(A-B) Isolated mouse primary hepatic stellate cells (HSC) were cultured for 4 days, and then treated with conditioned media (CM) from cholangiocytes, with or without OPN-targeted RNA aptamers for 48 hrs. (C-D) In separate experiments, primary HSC were directly treated with recombinant OPN (rOPN: 0 or 100ng/ml) for 24 hrs, and then harvested for QRT-PCR analysis. (A, C.) α sma, (B, D) collagen mRNA. Mean \pm SEM of duplicate experiments are graphed. *P<0.05 vs. vehicle treated stellate cells.

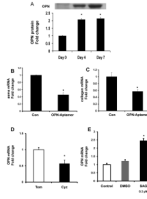


Figure 4. Hh-regulated OPN overexpression promotes HSC activation in an autocrine fashion
 Rat primary HSC were isolated and cultured for 0, 4 and 7 days. At the end of treatment, HSC were washed and cell lysates obtained for Western blot analysis. (A) OPN Western blot and densitometry. In separate experiments, day 4 HSC cultures were treated with OPN-aptamers or null-aptamers (control) for 48 hrs and RNA isolated for QRT-PCR (B-C). (B) α sma, (C) collagen mRNA. To assess if OPN expression is Hh-regulated, day 4 HSC were treated with Cyclopamine (Cyc), Tomatidine (Tom), or SAG for 24 hrs, and then harvested for RNA analysis (D-E). (D-E) opn mRNA. Mean \pm SEM of duplicate experiments are graphed. * $p < 0.05$ vs. control (vehicle) treated or quiescent stellate cells.

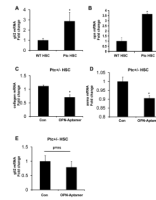


Figure 5. OPN is a downstream target of the Hh pathway

WT and Ptc^{+/-} primary HSC were placed in culture for 4 days and then harvested for RNA analysis by QRT-PCR. (A) gli2, (B) opn mRNA; mean ± SEM of duplicate experiments are graphed. *p<0.05 vs. WT HSC. In separate experiments, Ptc^{+/-} HSC were treated with OPN-aptamers or null-aptamers (control) for 48hrs, and effects on fibrogenesis assessed by QRT-PCR. (C) collagen, (D) αsma, and (E) gli2 mRNA. Mean ± SEM of triplicate experiments are graphed. * p<0.05 vs. null-aptamer-(control) treated HSC

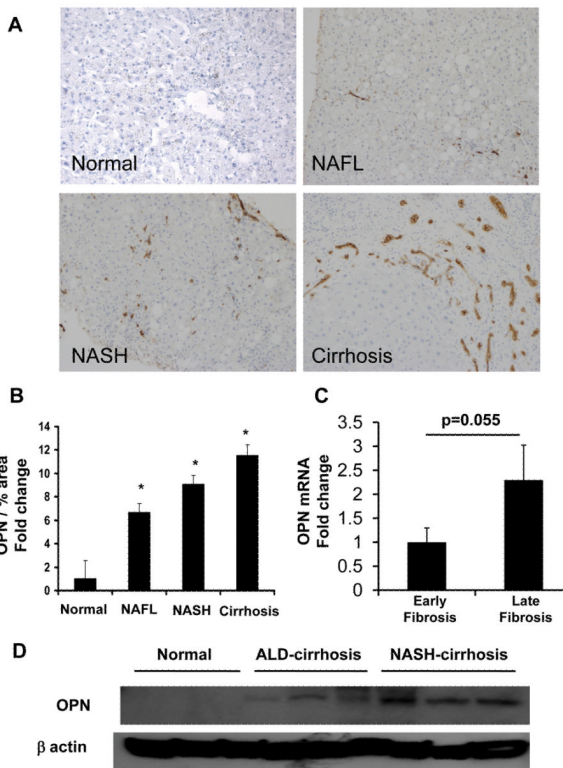


Figure 6. OPN over-expression in NAFLD patients

Coded liver sections from patients with NAFL, NASH, and NASH-cirrhosis were stained for OPN and analyzed by computer-assisted morphometry. (A) Representative photomicrographs of liver sections from patients with NAFLD and normal liver from excess donor tissues (400X). (B) Quantitative analysis of OPN in all patients. Amount of OPN is expressed as percentage of stained cells per high-powered field. * $P < 0.05$ vs. normal. Total liver RNA was isolated from individuals ($n=18$ /group) with early or late NASH-fibrosis and analyzed by QRT-PCR. (C) opn mRNA. Mean \pm SEM are graphed * $p < 0.05$ vs early fibrosis. (D) Hepatic OPN protein from normal, ALD-cirrhosis and NASH-cirrhosis individuals

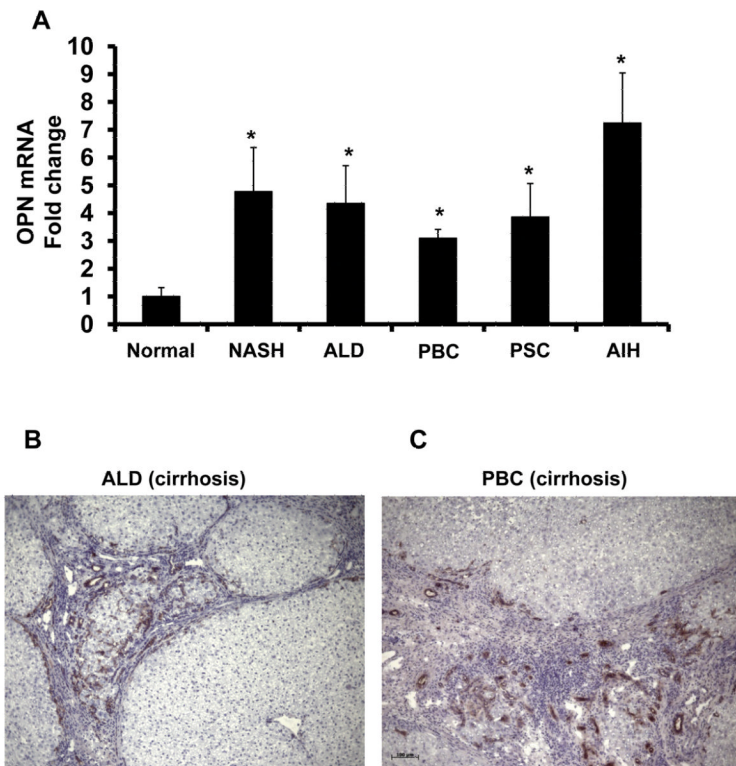


Figure 7. Enrichment of hepatic OPN in patients with chronic liver disease

RNA were harvested from explanted ALD-, NASH-, PBC-, PSC- and AIH-cirrhotic livers and analyzed by QRT-PCR. Liver sections from ALD and PBC-cirrhosis were immunostained for OPN. (A) OPN mRNA (n=6/group); results expressed as fold change relative to normal donor livers, mean \pm SEM. * $p < 0.05$ vs. normal. (B) Representative OPN immunostaining in ALD-cirrhosis (100X), and (C) PBC-cirrhosis (100X).